PHYSICAL REVIEW E VOLUME 52, NUMBER 4 OCTOBER 1995

Smectic-A and smectic-A_2 phases in aligned cylinders with a cylindrical attractive square well at one end

Richard P. Sear* and George Jackson†
Department of Chemistry, University of Sheffield, Sheffield, S3 7HF, United Kingdom

(Received 29 November 1994)

Nematic (N), smectic-A (Sm-A), and bilayer smectic-A_2 (Sm-A_2) phases are studied for an aligned fluid of cylinders with a cylindrical attractive square well at one end. The smectic phases are treated using an extension of the theory of Hosino, Nakano, and Kimura [J. Phys. Soc. Jpn. **46**, 1709 (1979)]. The smectic-A_2 phase has a modulation in the probability of a molecule pointing up (or down) in addition to the density modulation of a smectic-A phase. As for the smectic-A density wave, this second modulation requires an order parameter. A theory including the two order parameters is developed and the phase diagram calculated. This phase diagram shows N–Sm-A, N–Sm-A_2, and Sm-A–Sm-A_2 phase transitions that are second order, first order, and second order at high temperature above a tricritical point and first order below, respectively. Somewhat surprisingly, there is also a Sm-A–Sm-A transition; this is bracketed by a critical point at high temperature and the Sm-A–Sm-A_2 transition at low temperature. There is thus a triple point where the Sm-A–Sm-A and Sm-A–Sm-A_2 transitions meet. The two coexisting Sm-A phases differ in both the density and the wavelength of the smectic density modulation. Also notable is the very weak dependence on temperature of the N–Sm-A transition, in contrast to earlier work on cylinders with saturable attractive forces such that only dimers form [R.P. Sear and G. Jackson, Mol. Phys. **83**, 961 (1994)].

PACS number(s): 61.30.−v, 64.60.Cn, 64.70.Md

I. INTRODUCTION

Liquid crystals, states of matter intermediate between the liquid and the solid, exist as a bewildering variety of phases [1]. The structures of many of these phases have been probed with techniques such as x-ray scattering and the information gained has been related to the structure of the component molecules to provide explanations for the formation of these phases. For example, the smectic-A (Sm-A) phase is relatively well understood [2]; here the molecules are preferentially aligned along one direction as in a nematic (N) liquid crystal and in addition form layers perpendicular to this direction (see Refs. [1,3] for a discussion of the structure of liquid crystalline phases). However, in 1979 a Sm-A–Sm-A transition was reported [4] implying the existence of two Sm-A phases; x-ray scattering showed two quasi-Bragg peaks of wave vectors k and $2k$ [5] on one side of the transition, but only one of wave vector $2k$ on the other. The larger wave vector $2k$ corresponded to a wavelength of about the length of a molecule, the typical wavelength for smectic-A layering. The presence of two strong peaks at the commensurate wave vectors k and $2k$ together with the presence of only one at $2k$ in the other Sm-A phase is suggestive of ordering both at length scales k^{-1} and $(2k)^{-1}$. Later experimental work observed a second-order transition between these phases [6], in agreement with symmetry arguments that a transition in which the period doubles is allowed to be second order [7]. The ordering at $(2k)^{-1}$ is then the usual Sm-A layering and the ordering at k^{-1} is interpreted as differing alternate layers, i.e., that the first, third, etc., layers are the same, but differ from the second, fourth, etc., layers. This has led to the phase being christened the bilayer smectic phase, or Sm-A_2. The molecules forming this phase have very different "heads" and "tails" and so it is possible that, say, the head-head interactions are energetically favorable. This would provide a driving force for alternating layers in which most of the molecules point up or down (see Fig. 1).

The first work to quantify these ideas was the Landau theory of Prost [8]; see also [9,10]. There the effect of two coupled modulations with wave vectors k and $2k$ and their corresponding order parameters was considered, and the phenomenology of the experimental phase diagram was well reproduced. A mean-field theory has also been examined by Longa and de Jeu [11]. By contrast, to our knowledge there has been no work for a particular molecular model. Without such a model, a theory is limited to describing only the phenomena, not the underlying molecular behavior in a particular phase. The situation is different if a molecular model is used in a theory that, although approximate, is based on well understood and controlled approximations. Even a theory that is only qualitative will yield information on the features of a molecule responsible for the formation of a particular phase. It is hoped that the theory presented here will give insight into the molecular features responsible for smectic-A polymorphism.

A microscopic theory may be particularly useful here because of the occasional use of dimerization [5] to de-

---

*Electronic address: R.P.Sear@sheffield.ac.uk
†Electronic address: G.Jackson@sheffield.ac.uk

1063-651X/95/52(4)/3881(11)/$06.00

scribe the head-head interaction. Dimerization implies that a head can interact with only one other head at a time, i.e., the interaction is saturable. Clearly, a molecular model and theory are necessary to consider the implications of a microscopic phenomenon such as dimerization. This contribution is concerned with a nonsaturable interaction, but our earlier work has considered dimerization [12], albeit with a different theoretical approach. The results for saturable and nonsaturable interactions will be compared in the Conclusion.

Another interesting but difficult point is whether it is feasible that a Sm-A_2 phase could form due to purely repulsive, i.e., excluded volume, interactions. Work on a simple nail shaped model [13,14] has shown the formation of a Sm-A_d phase. The Sm-A_2 and Sm-A_d phases differ only in wavelength; the Sm-A_d has a modulation of around 1.6 times the length of a molecule as opposed to 2 times for a Sm-A_2 phase. This similarity is masked to a certain extent by the presence of the two strong peaks at k and $2k$ for a Sm-A_2 phase but only the one peak for the Sm-A_d phase. Of course, in all smectic phases there are peaks at k, $2k$, $3k$, ... because these correspond to the fundamental, the first harmonic, the second harmonic, etc. [15]. However, the harmonics are usually too weak to be observed above the background noise. In the case of a Sm-A_2 phase, but not a Sm-A_d phase, the modulation in the total density is "nearly" a wave of wave vector $2k$; in fact, it has a wave vector $2k$ at a second-order Sm-A–Sm-A_2 transition, but when the order parameter for the modulation in the fraction of molecules pointing up or down is finite this ordering couples with the density modulation, causing the period of this modulation to double. The mechanism for this is seen in Fig. 1. In the Sm-A phase the number of heads in between any two adjacent layers is the same, but within the Sm-A_2 phase alternate pairs of layers have very many and very few heads lying between them. A pair of layers with many intervening heads will be pulled together, thus reducing the layer spacing, while the opposite effect will occur for a pair of layers with very few intervening heads. This, of course, means that the period of the modulation in the total density is now two not one of the layers. The effect of the attractive forces shrinking alternate layer spacings is expected to be small and if it is indeed small then the modulation in the total (i.e., irrespective of orientation) density will be close to that of wave vector $2k$ and will therefore have an unusually strong first harmonic.

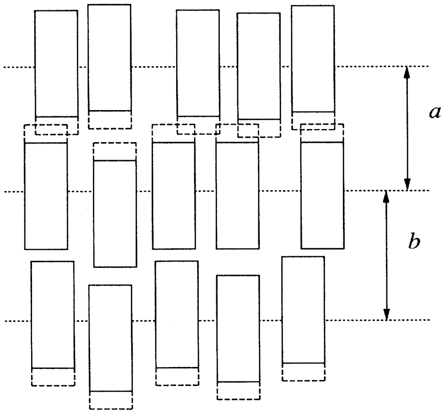

FIG. 1. The layering present in a Sm-A_2 phase is shown as alternating layers of molecules pointing up and down (see Fig. 2 for a description of the model molecule). The dotted lines indicate the centers of the layers. a and b indicate two different intervals: a is the layer spacing when the heads of the molecules are between the two adjacent layers and b is the layer spacing when the tails of the molecules are between the two layers.

Interestingly, a direct Sm-A_d–Sm-A_2 transition has been observed experimentally [16,1]. The transition ended at a critical point at which both the densities and the wavelengths of the two phases became equal. Above the critical temperature the Sm-A_d and Sm-A_2 phases are indistinguishable, just as a supercritical fluid does not have separate gas and liquid phases. This is not the only possibility; a similar Sm-A–Sm-A_d transition has been observed to end at an island of a nematic phase [17,18], i.e., around where the critical point should be there is a region where the equilibrium phase is nematic. In this context it is worthy of note that if the wavelength of a Sm-A_d phase decreases to around the length of a molecule, then the antiparallel ordering disappears, leaving a conventional Sm-A phase. Thus the Sm-A phase may transform directly to a Sm-A_2 phase by a first- or second-order transition or it may transform into a Sm-A_d phase (with or without a phase transition) and then, by further increasing the wavelength, into a phase we would classify as Sm-A_2 (again with or without a phase transition). This is unusual in the sense that normally two phases separated by a second-order transition can never transform from one to the other without a phase transition. Here, because the symmetry is determined by the wavelength of the modulation and this wavelength is a continuous variable even if a second-order transition is observed between a Sm-A and a Sm-A_2 phase, it is possible that we may be able to go from one phase to the other without passing through a phase transition; indeed this has been observed experimentally [19].

We have argued that the Sm-A_2 and Sm-A_d phases differ only in their wavelength, in an analogous way to the difference in density, which distinguishes the liquid and gas phases. However, with the purely repulsive nail shaped model of Hołyst [14], the wavelength at the transition is 1.56 times the molecular length and decreases with increasing density, thus we would always classify the phase as a Sm-A_d phase. It seems unlikely that a simple hard-core model will order with a wavelength that is twice its length.

In the following sections we first define a very simple model of a molecule with hard-core interactions favoring smectic-A ordering (see [20,15,3]) and an attractive interaction favoring bilayer formation. An approximate theory for the nematic and smectic phases of this model is then derived following [20]. The phase diagram calculated using this theory is presented and its broad features discussed. Finally, we conclude by putting the model and phase diagram into perspective.

II. MODEL AND THEORY

In contrast to earlier theoretical efforts to describe and understand the bilayer smectic, we use a specific model molecule. This model is perhaps the simplest representation of a molecule that might form a Sm-A_2 phase; it is shown in Fig. 2. The hard core of our molecule creates a volume surrounding it that is excluded to the other molecules; this effect alone has been shown to induce the nematic and smectic-A phases; see the reviews of Frenkel [3] and of Allen *et al.* [21]. In addition, if the attractive caps of two molecules overlap there is an energy ε released. The model is thus a particular case of an anisotropic generalization of the isotropic hard-sphere plus square-well potential used extensively in the study of simple fluids [22].

Theoretical study, even of simple cylindrical models, is complex for phases with positional ordering, such as the smectic-A (see Ref. [23] and references therein). So, in order to simplify the theory we consider only a fluid in which the molecules are aligned along the z axis. Thus the fluid has perfect nematic ordering at all densities. This clearly precludes the study of the isotropic-nematic and isotropic-smectic transitions; the fluid is, contrary to reality, nematic down to arbitrarily low densities. In addition, when the molecules are perfectly aligned the properties of the fluid becomes independent of the ratio L/D, where L defines the length scale of the z axis and D the length scale of the x and y axes. There is then only one model parameter: the ratio L_ε/L, where L_ε is the total length of the molecule including the square-well cap. The energy ε defines our temperature scale; the reduced temperature $T^* = k_B T/\varepsilon$, where T is the temperature and k_B is Boltzmann's constant.

If the model molecules are very long, the number density at the isotropic-nematic transition is $O(L^{-2}D^{-1})$ while the nematic-smectic and smectic-solid transition densities are $O(L^{-1}D^{-2})$. The nematic-smectic transition is thus deep into the nematic phase and the rods will be highly aligned. In this case the nematic-smectic transition seems to be quite close to that of the aligned system [24]. It may therefore be hoped that the phase diagram of an aligned system corresponds quite closely to that of the corresponding freely rotating system (excluding the latter's isotropic phase) provided L is large [25]. There is an exception to this as aligned systems may form columnar phases [12], but columnar phases have not been observed for freely rotating rods. It is likely that only very small deviations from perfect alignment are sufficient in long rods to destroy columnar ordering. The situation is very different for disks, although perfectly aligned disks behave in exactly the same way as rods; even very small fluctuations in the orientation of disks will destroy smectic ordering (but presumably not the columnar ordering).

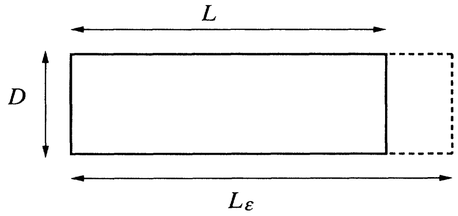

FIG. 2. Cross section of the model molecule. The model is a hard cylinder of length L and diameter D with an attractive cap at one end; the cap is cylindrical with the same diameter D and the total length of the molecule including this cap is L_ε. The center of the molecule is taken as the center of the hard cylinder.

We start from the free-energy functional truncated at the second virial coefficient level [22]

$$\beta A = \int \rho(1)\left\{\ln[\rho(1)\Lambda^3] - 1\right\} d(1) - \frac{1}{2}\int \rho(1)\rho(2) f(12) d(1) d(2) \tag{1}$$

for A the Helmholtz free energy. The number density $\rho(1)$ is given as a function of the coordinates (1), which represents both the position vector $\mathbf{r}$ and the orientation s. The spinlike variable s takes values ± 1: $+1$ if the molecule is parallel to the z axis and -1 if it is antiparallel to the z axis. Although the molecules are aligned with the z axis, they may be either parallel or antiparallel to it; this is different from the case of simple cylinders that are unchanged by rotation through π. The integrations in Eq. (1) are therefore integrations over position and sums over the spin variable. $\beta = 1/k_B T$ and Λ is the de Broglie wavelength of a molecule. The Mayer f function of the intermolecular potential is $f(12)$, where (12) represents the relative coordinates of molecules 1 and 2.

The potential function is a sum of two parts: the repulsive part modeled as a hard-core cylinder and the attractive cap. Using this, the Mayer f function may be factorized into two parts

$$f(12) = f_{\mathrm{HC}}(12) + e_{\mathrm{HC}}(12) f_a(12), \tag{2}$$

where $f_{\mathrm{HC}}(12)$ and $f_a(12)$ are the f functions of the hard core and the attractive cap, respectively, and $e_{\mathrm{HC}} = f_{\mathrm{HC}} + 1$. The f function of a hard-core potential is -1 if the two hard cores overlap and zero otherwise, and for a square-well attraction the f function is $\exp(\beta\varepsilon) - 1 = F$ when the wells overlap and again zero otherwise. So,

$$f_{\mathrm{HC}}(12) = -\mathcal{O}_{D,L}(\mathbf{r}_{12}), \tag{3}$$

$$f_a(12) = F\delta_{s,+1}\delta_{s',-1}\mathcal{O}_{D,L_\varepsilon}(\mathbf{r}_{12})H(z'-z) + F\delta_{s,-1}\delta_{s',+1}\mathcal{O}_{D,L_\varepsilon}(\mathbf{r}_{12})H(z-z'), \tag{4}$$

where $\mathcal{O}_{a,b}$ is an overlap function,

$$\mathcal{O}_{a,b}(\mathbf{r}_{12}) = H(a^2 - x_{12}^2 - y_{12}^2)H(b - |z_{12}|). \tag{5}$$

H is the step function, δ is the Kronecker delta, and $\mathbf{r}_{12} = \mathbf{r}' - \mathbf{r}$. The undashed and dashed coordinates refer to molecules 1 and 2, respectively. The Mayer f function Eq. (2) now becomes

$$
\begin{aligned}
f(12) = &-\mathcal{O}_{D,L}(\mathbf{r}_{12}) \\
&+F[\delta_{s,+1}\delta_{s',-1}H(z'-z) \\
&+\delta_{s,-1}\delta_{s',+1}H(z-z')] \\
&\times[\mathcal{O}_{D,L_\epsilon}(\mathbf{r}_{12}) - \mathcal{O}_{D,L}(\mathbf{r}_{12})]\,. \qquad (6)
\end{aligned}
$$

Substituting this in the free-energy functional Eq. (1)

$$
\begin{aligned}
\beta A = &\int \rho(1)\left\{\ln[\rho(1)\Lambda^3] - 1\right\} d(1) \\
&+\frac{1}{2}\int \rho(1)\rho(2)\mathcal{O}_{D,L}(\mathbf{r}_{12})d(1)d(2) \\
&-F\int \rho(1)\rho(2)\delta_{s,+1}\delta_{s',-1}H(z'-z) \\
&\times[\mathcal{O}_{D,L_\epsilon}(\mathbf{r}_{12}) - \mathcal{O}_{D,L}(\mathbf{r}_{12})]\,d(1)d(2). \qquad (7)
\end{aligned}
$$

The first of the two second virial coefficient integrals represents the contribution of excluded volume interactions. In the spirit of van der Waals we scale this term by an approximation to the free volume [26–28]

$$
\begin{aligned}
\beta A = &\int \rho(1)\left\{\ln[\rho(1)\Lambda^3] - 1\right\} d(1) + (1-\eta)^{-1}\int \rho(1)\rho(2)H(z'-z)\mathcal{O}_{D,L}(\mathbf{r}_{12})d(1)d(2) \\
&-F\int \rho(1)\rho(2)\delta_{s,+1}\delta_{s',-1}H(z'-z)\,[\mathcal{O}_{D,L_\epsilon}(\mathbf{r}_{12}) - \mathcal{O}_{D,L}(\mathbf{r}_{12})]\,d(1)d(2) \qquad (8)
\end{aligned}
$$

for $\eta = \rho v_0$ the volume fraction of the fluid, ρ is the average number density, and $v_0 = \pi L D^2/4$ is the volume of a molecule. The second virial coefficient has now been reduced to three integrals, each of the same form; the excluded volume integral has been converted to an integral over the space $z' > z$ by use of the fact that the overlap function is symmetric about $z' - z = 0$.

In the nematic phase the number density is a constant and the integrals are trivial; the free energy is then

$$
\frac{\beta A}{N} = \ln(\rho\Lambda^3) - 1 + 4\eta(1-\eta)^{-1} - F\eta\left(\frac{L_\epsilon}{L} - 1\right). \qquad (9)
$$

In order to estimate the free energy of the smectic-*A* phase we calculate the free energy in the presence of a square-wave density modulation, following Hosino *et al.* [20]. The form of the wave is illustrated in Fig. 3. In the Sm-*A* phase only the total density varies with position; the fraction of molecules with spin up is equal to the fraction with spin down at every point, as in the nematic phase. So, the number density is now a function of z, but not a function of x, y, or s:

$$
\rho(z) = \begin{cases} \rho\left(1 + \frac{q}{p}\sigma\right), & m\lambda \le z < m\lambda + p\lambda \\ \rho(1-\sigma), & m\lambda + p\lambda \le z < (m+1)\lambda, \end{cases} \qquad (10)
$$

where σ is the excess fraction of molecules in the "humps"; as such it varies from zero to one. It is the order parameter for the Sm-*A* phase. When σ is nonzero the fluid splits into layers of high and low density. The high-density layers we call type-*A* layers and the low-density layers type *B*. The wavelength is λ ($= 2\pi/k$), m is an integer, and $q\lambda$ and $p\lambda$ are the widths of the two types of layers; see Fig. 3. The integration over all coordinates except z in the free energy Eq. (8) is still trivial:

$$
\begin{aligned}
\frac{\beta A}{V} = &(\lambda)^{-1}\int_0^\lambda \rho(z)\left\{\ln[\rho(z)\Lambda^3] - 1\right\} dz + 4v_0(1-\eta)^{-1}(\lambda L)^{-1}\int_0^\lambda\int \rho(z)\rho(z')H(z'-z)H(L-z'+z)dzdz' \\
&-Fv_0(\lambda L)^{-1}\int_0^\lambda\int \rho(z)\rho(z')H(z'-z)\,[H(L_\epsilon - z' + z) - H(L - z' + z)]\,dzdz'. \qquad (11)
\end{aligned}
$$

The second integration in both of the second virial coefficient terms is unrestricted. Integration of the ideal gas term is simple, but the second virial coefficient is less straightforward; each of the three integrals there is the same so we consider only one of them

$$
(\lambda L)^{-1}\int_0^\lambda\int \rho(z)\rho(z')H(z'-z)H(L-z'+z)dzdz'. \qquad (12)
$$

The number density $\rho(z)$ may be replaced in Eq. (12) by an excess number density $\rho'(z)$, defined by

$$
\rho'(z) = \rho(z) - \rho(1-\sigma). \qquad (13)
$$

The second term may be identified as the number density in the type-*B* layers, thus the excess densities are zero in layers of type *B*. Substituting Eq. (13) in Eq. (12)

$$(\lambda L)^{-1}\int_0^\lambda\int\left[\rho'(z)\rho'(z')+2\rho(1-\sigma)\rho'(z)+\rho^2(1-\sigma)^2\right]H(z'-z)H(L-z'+z)dzdz' \tag{14}$$

$$\begin{aligned}&=(\rho\sigma/p)^2(\lambda L)^{-1}\int_0^{p\lambda}\int_A H(z'-z)H(L-z'+z)dzdz'\\&\quad+2\rho^2\sigma(1-\sigma)/p(\lambda L)^{-1}\int_0^{p\lambda}\int H(z'-z)H(L-z'+z)dzdz'\\&\quad+\left[\rho(1-\sigma)\right]^2(\lambda L)^{-1}\int_0^{\lambda}\int H(z'-z)H(L-z'+z)dzdz'.\end{aligned} \tag{15}$$

The subscript A on an integration sign indicates that the integration is restricted to within layers of type A. It is only the first integral where both molecules are restricted to within the layers of type A, which is nontrivial. We represent this integral by $2I^{AA}(\kappa,p)$: it is a function only of $\kappa=\lambda/L$, the ratio of the wavelength to L, and p. The factor of 2 is for consistency with the integrals for the bilayer phase. This integral and the others found for the bilayer phase are evaluated in the Appendix. We then have, after a little algebra,

$$\rho^2\left[1+\sigma^2\left(\frac{2I^{AA}(\kappa,p)}{p^2}-1\right)\right]. \tag{16}$$

Inserting this in the free energy

$$\begin{aligned}\frac{\beta A}{N}&=\ln\rho\Lambda^3-1+(p+q\sigma)\ln(1+q\sigma/p)+q(1-\sigma)\ln(1-\sigma)+4\eta(1-\eta)^{-1}\left[1+\sigma^2\left(\frac{2I^{AA}(\kappa,p)}{p^2}-1\right)\right]\\&\quad-F\eta\left[\frac{L_\epsilon}{L}-1+\sigma^2\left(\frac{L_\epsilon}{L}\frac{2I^{AA}(\kappa_\epsilon,p)}{p^2}-\frac{2I^{AA}(\kappa,p)}{p^2}-\frac{L_\epsilon}{L}+1\right)\right],\end{aligned} \tag{17}$$

where $\kappa_\epsilon=\lambda/L_\epsilon$. At a given temperature and density the free energy of the Sm-A phase depends on the three parameters σ, κ, and p. At equilibrium the free energy will be at a minimum with respect to variations in these parameters; this criterion defines the equilibrium values of the parameters.

In both the nematic phase and in the smectic-A phase the fraction of molecules pointing up (say) is uniform: it is equal to $\frac{1}{2}$. At a second-order Sm-A–Sm-A_2 phase transition this fraction of molecules pointing in one direction acquires a modulation of twice the period of the modulation in the total density. The coupling of this spin wave to the density wave then causes the period of the density wave to double. The density is a function of z and s

$$\rho(1)=\rho(z,s)=\rho(z)[\delta_{s,+1}f_+(z)+\delta_{s,-1}f_-(z)], \tag{18}$$

where $f_+(z)$ and $f_-(z)$ are the fractions of molecules with the attractive cap above ($s=+1$) and below ($s=-1$) the center of the molecule, respectively. This factorization of the density into the total density times a factor that depends on s is perfectly general. Both $\rho(z)$ and $f_+(z)$ have the same period, but if we assume that bilayer formation has a small effect on the layer spacing of alternate pairs of layers then it is reasonable to neglect this effect and retain the Sm-A form of $\rho(z)$ given by Eq. (10). It is important to note that using a $\rho(z)$ with a period half that of $f_+(z)$ is an approximation and not a feature of the symmetry of the Sm-A_2 phase (except along a second-order transition from a Sm-A phase). In addition, by removing part of the coupling between the density and spin modulations the tendency of the Sm-A–Sm-A_2 transition towards becoming first order may be underestimated.

The variation in $f_+(z)$ and $f_-(z)$ with position is again approximated by a square wave, but here, due to symmetry, the two types of layers, called a and b, are of the

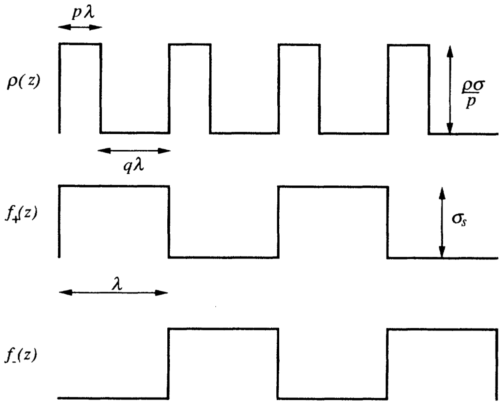

FIG. 3. Square-wave density modulations in the Sm-A and Sm-A_2 phases. The top wave $\rho(z)$ is the density modulation in the Sm-A and Sm-A_2 phases. The middle wave $f_+(z)$ is the modulation in the fraction of molecules pointing up (i.e., with $s=+1$) present in the Sm-A_2 phase and the bottom wave $f_-(z)$ is the equivalent of $f_+(z)$ for downward pointing molecules. The symbols are defined in the text.

same width; see Fig. 3. This symmetry follows from the fact that the two functions $f_{+}(z)$ and $f_{-}(z)$, which sum to unity, are equivalent:

$$f_{+}(z)=\begin{cases}\frac{1}{2}(1+\sigma_s)\,, & 2m\lambda\le z<(2m+1)\lambda\\ \frac{1}{2}(1-\sigma_s)\,, & (2m+1)\lambda\le z<2(m+1)\lambda,\end{cases} \tag{19}$$

$$f_{-}(z)=\begin{cases}\frac{1}{2}(1-\sigma_s)\,, & 2m\lambda\le z<(2m+1)\lambda\\ \frac{1}{2}(1+\sigma_s)\,, & (2m+1)\lambda\le z<2(m+1)\lambda,\end{cases} \tag{20}$$

where σ_s is the order parameter for the Sm-A_2 phase. When σ_s is nonzero the smectic layers are alternately rich in one orientation and then rich in the other. The decrease in entropy caused by this loss in orientational freedom is compensated by the energy released by more of the attractive caps overlapping. Clearly, if a layer of molecules pointing up is directly below one of molecules pointing down, the opportunities for overlap of these caps are greatly increased; the caps on two molecules can only overlap when the molecules are antiparallel, due to the hard cores. Smectic ordering is driven by the reduction in volume excluded to a molecule when alternating layers of high and low density are formed; this leads to a density modulation with a wavelength a little longer than the length of the molecule. The formation of bilayers is driven by the energy released when the molecules of two adjacent layers point towards each other and many of their attractive square wells overlap. The characteristic modulation is then of a wavelength around twice the range of the attraction, with the modulations in the two orientations in antiphase.

The free energy Eq. (8) may be simply integrated over all coordinates except z:

$$\begin{aligned}\frac{\beta A}{V}&=2(2\lambda)^{-1}\int_0^{2\lambda}\rho(z)f_{+}(z)\left\{\ln[\rho(z)f_{+}(z)\Lambda^3]-1\right\}dz\\ &\quad+4v_0(1-\eta)^{-1}(2\lambda L)^{-1}\int_0^{2\lambda}\int\rho(z)\rho(z')H(z'-z)H(L-z'+z)dzdz'\\ &\quad-4Fv_0(2\lambda L)^{-1}\int_0^{2\lambda}\int\rho(z)f_{+}(z)\rho(z')f_{-}(z')H(z'-z)\left[H(L_\epsilon-z'+z)-H(L-z'+z)\right]dzdz'.\end{aligned} \tag{21}$$

Here, the two equivalent ideal gas terms for the two orientations have been combined, and in the excluded volume term the irrelevant dependence on f_{+} and f_{-} has been summed over. The two equivalent terms in the attractive part of the second virial coefficient have also been added together.

In an analogous way to our definition of the excess number densities in Eq. (13), we define excess fractions of the two orientations as

$$f'_{+}(z)=f_{+}(z)-\frac{1}{2}(1-\sigma_s), \tag{22}$$

with an equivalent definition for $f'_{-}(z)$. Substituting these excess fractions into the first of the two attractive integrals of Eq. (21)

$$(2\lambda L)^{-1}\int_0^{2\lambda}\int\rho(z)\rho(z')\left[f'_{+}(z)f'_{-}(z')+(1-\sigma_s)f'_{+}(z)+\frac{1}{4}(1-\sigma_s)^2\right]H(z'-z)H(L_\epsilon-z'+z)dzdz', \tag{23}$$

the second integral is exactly the same except for the substitution of L for L_ϵ. Continuing, we write

$$\begin{aligned}&\sigma_s^2(2\lambda L)^{-1}\int_0^{\lambda}\int_b\rho(z)\rho(z')H(z'-z)H(L_\epsilon-z'+z)dzdz'\\ &\quad+\sigma_s(1-\sigma_s)(2\lambda L)^{-1}\int_0^{\lambda}\int\rho(z)\rho(z')H(z'-z)H(L_\epsilon-z'+z)dzdz'\\ &\quad+\frac{1}{4}(1-\sigma_s)^2(2\lambda L)^{-1}\int_0^{2\lambda}\int\rho(z)\rho(z')H(z'-z)H(L_\epsilon-z'+z)dzdz'.\end{aligned} \tag{24}$$

A subscript b on an integration indicates that the integration is restricted to layers of type b. In Eq. (24) the terms linear in σ_s cancel as they should; symmetry forbids such terms. Then subtracting the second term from the first

$$\begin{aligned}&-\sigma_s^2(2\lambda L)^{-1}\int_0^{\lambda}\int_a\rho(z)\rho(z')H(z'-z)H(L_\epsilon-z'+z)dzdz'\\ &\quad+\frac{1}{4}(1+\sigma_s^2)(2\lambda L)^{-1}\int_0^{2\lambda}\int\rho(z)\rho(z')H(z'-z)H(L_\epsilon-z'+z)dzdz'.\end{aligned} \tag{25}$$

The second of these two integrals is just Eq. (12) and has already been dealt with. The first integral depends on both the density and the spin waves and it is the only part of the free energy that depends on their relative phase. The excess density Eq. (13) is substituted in the first integral of Eq. (25) to give

$$(2\lambda L)^{-1}\int_0^{\lambda}\int_a\left[\rho'(z)\rho'(z')+2\rho(1-\sigma)\rho'(z)+\rho^2(1-\sigma)^2\right]H(z'-z)H(L_\varepsilon-z'+z)dzdz' \tag{26}$$

$$\begin{aligned}&=\frac{\rho^2\sigma^2}{p^2}(2\lambda L)^{-1}\int_0^{p\lambda}\int_{aA}H(z'-z)H(L_\varepsilon-z'+z)dzdz'\\&\quad+2\frac{\rho^2\sigma(1-\sigma)}{p}(2\lambda L)^{-1}\int_0^{p\lambda}\int_a H(z'-z)H(L_\varepsilon-z'+z)dzdz'\\&\quad+\rho^2(1-\sigma)^2(2\lambda L)^{-1}\int_0^{\lambda}\int_a H(z'-z)H(L_\varepsilon-z'+z)dzdz'.\end{aligned} \tag{27}$$

A subscript aA means that the integration is restricted to regions (i.e., values of z) that are both in layers of type a and type A. The integrals are represented as functions of κ_ε and p:

$$\frac{\rho^2\sigma^2}{p^2}I^{aAaA}(\kappa_\varepsilon,p)+2\frac{\rho^2\sigma(1-\sigma)}{p}I^{aAa}(\kappa_\varepsilon,p)+\rho^2(1-\sigma)^2I^{aa}(\kappa_\varepsilon,p). \tag{28}$$

The I's are the integrals and the superscripts indicate the regions to which the integration is restricted. These integrals are all in the Appendix, together with a sketch of the derivation of the ideal gas term. The free energy is then

$$\begin{aligned}\frac{\beta A}{N}&=\ln\rho\Lambda^3-1+(p+q\sigma)\ln(1+q\sigma/p)+q(1-\sigma)\ln(1-\sigma)+\frac{1}{2}(1+\sigma_s)\ln(1+\sigma_s)\\&\quad+\frac{1}{2}(1-\sigma_s)\ln(1-\sigma_s)+4\eta(1-\eta)^{-1}\left[1+\sigma^2\left(\frac{2I^{AA}(\kappa,p)}{p^2}-1\right)\right]\\&\quad-F\eta\left\{\frac{L_\varepsilon}{L}-1+\sigma^2\left(\frac{L_\varepsilon}{L}\frac{2I^{AA}(\kappa_\varepsilon,p)}{p^2}-\frac{2I^{AA}(\kappa,p)}{p^2}+1-\frac{L_\varepsilon}{L}\right)\right.\\&\quad+\sigma_s^2\left(-4\frac{L_\varepsilon}{L}I^{aa}(\kappa_\varepsilon,p)+4I^{aa}(\kappa,p)+\frac{L_\varepsilon}{L}-1\right)\\&\quad+8\sigma_s^2\sigma\left[\frac{L_\varepsilon}{L}\left(I^{aa}(\kappa_\varepsilon,p)-\frac{I^{aAa}(\kappa_\varepsilon,p)}{p}\right)-I^{aa}(\kappa,p)+\frac{I^{aAa}(\kappa,p)}{p}\right]\\&\quad+\sigma_s^2\sigma^2\left[\frac{L_\varepsilon}{L}\left(\frac{2I^{AA}(\kappa_\varepsilon,p)-4I^{aAaA}(\kappa_\varepsilon,p)}{p^2}+\frac{8I^{aAa}(\kappa_\varepsilon,p)}{p}-4I^{aa}(\kappa_\varepsilon,p)-1\right)\right.\\&\quad\left.\left.-\frac{2I^{AA}(\kappa,p)-4I^{aAaA}(\kappa,p)}{p^2}-\frac{8I^{aAa}(\kappa,p)}{p}+4I^{aa}(\kappa,p)+1\right]\right\}.\end{aligned} \tag{29}$$

It is easy to verify that this expression for the free energy of the Sm-A_2 phase reduces to that for the Sm-A phase Eq. (17) when $\sigma_s=0$ and to that for the N phase Eq. (9) when both $\sigma_s=0$ and $\sigma=0$. In the limit of temperature tending to infinity only the hard-core interactions contribute (thus σ_s will be zero) and the free energy will reduce to that of Hosino *et al.* [20]. At a given temperature and density the equilibrium free energy is found by varying the four parameters σ, σ_s, λ, and p until the free energy Eq. (29) is a minimum. The pressure is the volume (or density) derivative of the free energy at constant temperature [29] and may thus be obtained by numerically differentiating the equilibrium free energy. The chemical potential of a pure component is just the Gibbs free energy per particle and may be obtained via the familiar thermodynamic relation $\mu=(A+PV)/N$.

III. PHASE DIAGRAM

Symmetry allows the N–Sm-A and Sm-A–Sm-A_2 transitions to be second order [7]; note the absence of linear terms in σ in Eq. (17) and in σ_s in Eq. (29) and also that there is no cubic term in σ_s, or in σ if $p=1/2$. Finding a second-order transition is a matter of finding the point where the order parameter is first nonzero at equilibrium. Finding this density at a given temperature simply requires a bisectionlike search of the density where σ or σ_s first becomes nonzero. For a first-order transition the two densities at coexistence are required; these are defined by the equalities of chemical potential and pressure. These two equalities form two equations in the two unknowns, i.e., the two densities, and the resulting two simultaneous equations are solved as in earlier work [30].

The pressure-temperature projection of the phase diagram for $L_\varepsilon/L = 1.2$ is shown in Fig. 4. First, we discuss the unsurprising features. The N–Sm-A transition is always second order, but the Sm-A–Sm-A_2 transition becomes first order as it approaches the N–Sm-A transition. As the pressure of the Sm-A–Sm-A_2 transition decreases the Sm-A ordering at the transition decreases, and once the Sm-A ordering is sufficiently far from saturation, the coupling between σ_s and σ drives the Sm-A–Sm-A_2 transition to become first order [31,8]. This occurs at a tricritical point in the Sm-A–Sm-A_2 transition [7]. Surprisingly, there is a Sm-A–Sm-A transition. As may be seen from the temperature-density projection, Fig. 5, there is a narrow, highly pointed coexistence region. This region is bounded by a critical point at high temperature and this coexistence region meets the Sm-A–Sm-A_2 coexistence region at a triple point at low temperature. The phase diagram for $L_\varepsilon/L = 1.05$, i.e., a much shorter ranged square well, has also been calculated and there the Sm-A–Sm-A coexistence region is moved towards the tricritical point, which is now at a density above close packing.

In Fig. 6 the behavior of the parameters of the free energy is displayed for a constant temperature slice, which includes the Sm-A–Sm-A transition. All four have a discontinuity within the coexistence region; the pressure isotherm (not shown) is also discontinuous. This is characteristic of a change in the global minimum of the free energy as a function of the four parameters [12]; at the discontinuity what was a local minimum becomes the global minimum. These two minima correspond to two competing wavelengths [8] for the Sm-A density wave. The discontinuity is very close to $\kappa = 1.2$, where the wavelength equals the total length of the model. It is perhaps necessary to be cautious about this prediction as both the potential and the density wave are step functions; the free energy may therefore be unrealistically sensitive to λ for $\lambda \approx L_\varepsilon$.

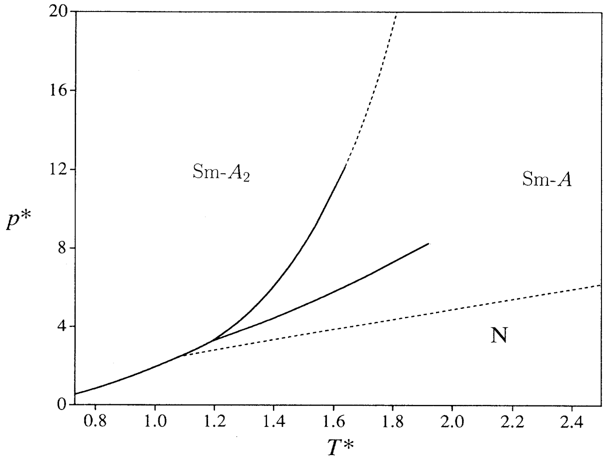

FIG. 4. Pressure-temperature projection of the phase diagram within our approximate theory for our model with $L_\varepsilon/L = 1.2$. The reduced pressure $p^* = Pv_0/\varepsilon$, where P is the pressure, and the reduced temperature $T^* = k_BT/\varepsilon$. The continuous and dashed curves indicate first- and second-order transitions, respectively.

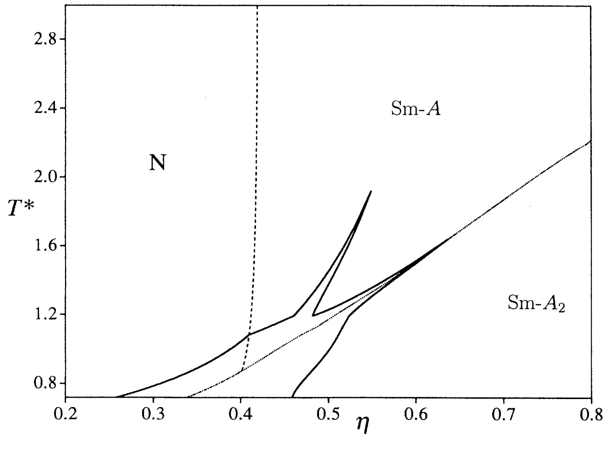

FIG. 5. Temperature-density projection of phase diagram for the system of Fig. 4., i.e., $L_\varepsilon/L = 1.2$. The continuous curve encloses the two-phase coexistence region while the dashed curve marks the first appearance of a nonzero σ at equilibrium and the dotted curve the first appearance of a nonzero σ_s.

The Sm-A–Sm-A critical point is closely analogous to critical points found in experiment [16,17] and with Landau theory [18] between two phases, which may be classified as Sm-A_d. In experiment, although some systems possessed this critical point [16], in others the critical point of the transition was masked by an island in the phase diagram where the nematic phase is the most stable phase [17]. The Landau theory used [18] did not predict this nematic island, but when a fluctuation corrected mean-field theory was used a nematic region appeared for certain parameter values [18]. There the melting of the smectic phase into the nematic was mediated by the un-

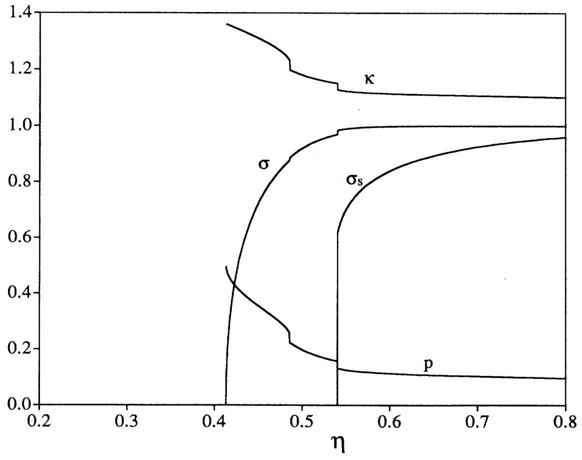

FIG. 6. Four parameters σ, σ_s, κ, and p are plotted as a function of density for a reduced temperature $T^* = 1.3$, again for the system $L_\varepsilon/L = 1.2$.

binding of dislocations. The absence of a nematic island in our phase diagram, Fig. 4, may be due to the model or to the approximations of the theory.

In order to look more closely at the effect of the attractive forces on the fluid in the smectic phases, the density dependence of the parameters at $T^* = 2$ and $T^* = \infty$, i.e., the hard-core limit, are compared in Fig. 7. Somewhat surprisingly, the effect of the attractive forces on the Sm-A ordering is slight; this is consistent with the very weak dependence of the N–Sm-A transition density on temperature seen in Fig. 5. The parameters κ and p are more sensitive to temperature; in particular they both show an undulation for $T^* = 2$ because this is only just above the critical temperature of the Sm-A–Sm-A transition $T^* = 1.92$. At the lower temperature of $T^* = 1.3$ (see Fig. 6) κ and p are more influenced by the attractive interactions. It may be seen that over a wide range of density the wavelength κ is close to 1.1 while p is a little above 0.1; it is easy to verify that for a wave with these values of κ and p the energy is near the minimum possible. An unrelated but interesting observation is that very near the tricritical point of the Sm-A–Sm-A_2 transition, σ_s is continuous, i.e., there is no jump, unlike that seen in Landau theory right up to the tricritical point.

The relative phase angle φ between the density and spin waves has been fixed at zero or π, depending on whether f_+ or f_- is used to define it. In the earlier work on a Sm-A_d phase [14] the phase angle was important, and nonzero. So now, after the fact, some justification is provided for the neglect of φ. The first integral of Eq. (25) is the only integral that depends on φ; it is non-negative and for our model it appears in the free energy as L_ϵ times its value for a cylinder of length L_ϵ minus L times its value for a cylinder of length L; this difference is also non-negative. The difference appears in the free energy multiplied by $+\sigma_s^2$ and so for nonzero σ_s, the free energy is minimized by the minimum value of this integral. Thus the equilibrium value of φ is that which minimizes this difference. Now, *if* $\sigma = 1$ then the difference is zero for $\varphi = 0$ (in fact for a range of φ), as seen in Eq. (29). The free energy for $\varphi = 0$ is therefore the equilibrium free energy. In the Sm-A_2 phase σ is always close to one; see Figs. 6 and 7.

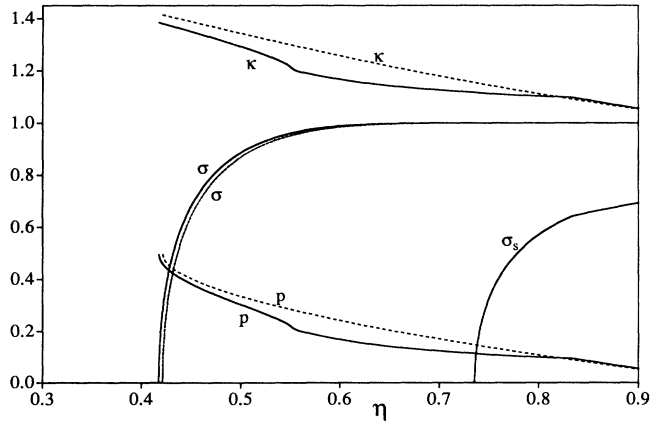

FIG. 7. Four parameters σ, σ_s, κ, and p are plotted as a function of density for a reduced temperature $T^* = 2$; $L_\epsilon/L = 1.2$. These are the solid curves. The high temperature limit is also plotted for comparison: σ, κ, and p are shown as dashed curves.

IV. CONCLUSION

A model molecule has been proposed and, using an approximate theory for an aligned fluid of these molecules, a rich phase diagram has been calculated. Aligning the molecules to the z axis is a reasonable approximation only for very long rods at packing fraction η of order unity. Thus it may be hoped that the phase diagram of Figs. 3 and 4 is a reasonable approximation to that of the freely rotating model if $L/D \gg 1$. However, the solid phase is missing from our calculated phase diagram. The aligned system will presumably undergo a smectic-solid transition and the density of this transition is unlikely to vary much with temperature (as for the N–Sm-A transition) being driven by excluded volume interactions. The smectic-solid transition for our model in the infinite temperature limit is weakly first order; the smectic density at coexistence is $\eta = 0.57$ according to simulation [32]. This suggests that the tricritical point and the second order Sm-A–Sm-A_2 transition is masked by the solid phase. Note that due to the scaling of the repulsive terms of the second virial coefficient our theory predicts a N–Sm-A transition at $\eta = 0.421$, in quite good agreement with the simulation result of $\eta = 0.44$ for the purely repulsive system.

In Fig. 4 the pressure at the nematic-smectic transition, whether it be to the Sm-A or Sm-A_2 phase, decreases monotonically as the temperature decreases. In contrast, earlier work on the nematic-smectic transition in a system of dimerizing cylinders [12], i.e., where the attractive interaction is saturable, showed that the transition pressure went through a maximum. In Ref. [12] different approximations were made; a bifurcation analysis was performed with respect to a sinusoidal perturbation. The Sm-A_2 phase was not considered and the treatment of dimers as a single molecule meant that what are three-body interactions between both molecules of a dimer and another monomer were included. Here, the simple treatment at the level of the second virial coefficient ignores interactions between a pair of molecules interacting via their square wells and another molecule. In [12] it is the monomer-dimer interactions that destabilize the smectic phase causing the maximum in the pressure of the nematic-smectic transition. We should therefore be cautious about the slowly varying pressure at the nematic-smectic transition found here. However, at low temperatures a fluid will adopt configurations with a low energy. For the nonsaturable interactions treated here, this means (antiparallel) layering due to the collective nature of the attractive interactions, whereas for saturable interactions the low-energy state of virtually complete bonding into dimers does not imply layering. A definitive description of the phase behavior of rods with saturable and with nonsaturable attractive interactions would require treating both with a much more accurate theory or computer simulation. Also, it would be necessary to account for the different ranges of the interactions: the dimerization interaction has been assumed to have zero range while the phase diagram presented here is for a square well that is 0.2 times as long as the hard core. Increasing the range of the interaction allows the molecules to interact without disrupting the layering.

ACKNOWLEDGMENTS

It is a pleasure for R.P.S. to acknowledge useful discussions with Blandine Jérôme and with Daan Frenkel, who pointed out the possibility of a nematic island surrounding the Sm-A–Sm-A critical point. One of us (R.P.S.) would like to thank the EPSRC and British Petroleum. We also acknowledge support from the Computational Initiative of the SERC (Grant No. GR/H58810-C91) for computer hardware.

APPENDIX

In this appendix the integrals required are evaluated as a function of κ (or κ_ε) and p. It is found that the integrals are required only in the range $1/2 \le \kappa \le 2$, the minimum of the free energy always lies at a wavelength within this range. Thus the integrals are calculated assuming κ is within this range. All the integrals are of the same form, i.e., that of integration of a step function over z and z'; thus we show explicitly only the calculation of one:

$$I^{aAa}(\kappa,p) = (2\lambda L)^{-1}\int_0^{p\lambda} dz \int_a dz' \times H(z'-z)H(L-z'+z).$$

In the remainder of this appendix the explicit dependence on κ and p is dropped. For $\kappa \ge 1$ and $q\kappa \le 1$,

$$\begin{aligned} I^{aAa} &= (2\lambda L)^{-1}\left(\int_0^{\lambda-L} dz \int_z^{z+L} dz' + \int_{\lambda-L}^{p\lambda} dz \int_z^{\lambda} dz'\right), \\ &= (2\lambda L)^{-1}\left(\lambda L - \frac{1}{2}L^2 - \frac{1}{2}q^2\lambda^2\right) \\ &= \frac{1}{2}\left(1 - \frac{1}{2\kappa} - \frac{1}{2}q^2\kappa\right). \end{aligned}$$

Furthermore,

$$I^{aAa} = \begin{cases} \dfrac{p}{2}, & \kappa \ge 1, q\kappa \ge 1 \\ \dfrac{1}{4}\kappa(1-q^2), & \kappa \le 1, (1+q)\kappa \ge 1. \end{cases}$$

The other integrals are

$$\begin{aligned} I^{AA} &= I^{aAaA} + I^{aAbA}, \\ I^{aAaA} &= \frac{1}{4}p^2\kappa, \quad p\kappa \le 1, (1+q)\kappa \ge 1, \\ I^{aAbA} &= \begin{cases} \dfrac{(1-q\kappa)^2}{4\kappa}, & q\kappa \le 1, \kappa \ge 1 \\ \dfrac{1}{4}[(1+p)\kappa - 1](1/\kappa - q) + \dfrac{1}{2}p(1-\kappa), & \kappa \le 1, (1+q)\kappa \ge 1 \\ \dfrac{1}{2}p^2\kappa, & (1+p)\kappa \le 1 \\ 0, & q\kappa \ge 1, \end{cases} \\ I^{aa} &= \begin{cases} \dfrac{1}{2}\left(1 - \dfrac{1}{2\kappa}\right), & \kappa \ge 1 \\ \dfrac{1}{2}\left(\kappa - 1 + \dfrac{1}{2\kappa}\right), & \kappa \le 1. \end{cases} \end{aligned}$$

The derivation of the ideal gas term in the Sm-A_2 phase is now sketched. The term in question is

$$(2\lambda)^{-1}\int_0^{2\lambda} dz \rho(z) f_+(z) \ln \rho(z) f_+(z).$$

The logarithm may be expanded as a sum of logarithms of ρ and f_+ giving two integrals

$$\frac{1}{2}(\lambda)^{-1}\int_0^{\lambda} dz \rho(z) \ln \rho(z) + \rho(2\lambda)^{-1}\int_0^{2\lambda} dz f_+(z) \ln f_+(z).$$

The $f_+(z)$ has disappeared from the first integral because it is constant over the period of the density modulation and averages to $\frac{1}{2}$ over 2λ. The $\rho(z)$ has disappeared from the second because it averages out to ρ over any period of length λ. Substituting Eqs. (10) and (19) into the equation then leads to the ideal gas part of Eq. (29).

[1] S. Chandrashekar, *Liquid Crystals*, 2nd ed. (Cambridge University Press, Cambridge, 1992).

[2] J. Prost, Adv. Phys. **33**, 1 (1984).

[3] D. Frenkel, in *Liquids, Freezing and Glass Transitions*, Proceedings of the Les Houches Summer School of Theoretical Physics, 1989, edited by J.-P. Hansen *et al.* (North-Holland, Amsterdam, 1991).

[4] G. Sigaud, F. Hardouin, M. F. Achard, and H. Gasparoux, J. Phys. (Paris) Colloq. **40**, C3-356 (1979).

[5] F. Hardouin, A. M. Levelut, J. J. Benattar, and G. Sigaud, Solid State Commun. **33**, 337 (1980).

[6] K. K. Chan, P. S. Pershan, L. B. Sorensen, and F. Hardouin, Phys. Rev. Lett. **54**, 1694 (1985).

[7] E.M. Lifschitz and L.P. Pitaevskii, *Statistical Physics*, 3rd ed. (Pergamon, Oxford, 1980).

[8] J. Prost, J. Phys. (Paris) **40**, 581 (1979).

[9] J. Prost and P. Barois, J. Chim. Phys. **80**, 65 (1983).

[10] P. Barois, J. Prost, and T. C. Lubensky, J. Phys. (Paris), **46**, 391 (1985).

[11] L. Longa and W. H. de Jeu, Phys. Rev. A **28**, 2380 (1983).

[12] R. P. Sear and G. Jackson, Mol. Phys. **83**, 961 (1994).

[13] M. Nakagawa and T. Akahane, J. Phys. Soc. Jpn. **56**, 2653 (1987).

[14] R. Hołyst, Phys. Rev. A **42**, 3438 (1990).

[15] B. Mulder, Phys. Rev. A **35**, 3095 (1987).

[16] R. Shashidhar, B. R. Ratna, S. Krishna Prasad, S. Somasekhara, and G. Heppke, Phys. Rev. Lett. **59**, 1209 (1987).

[17] P. E. Cladis and H. R. Brand, Phys. Rev. Lett. **52**, 2261 (1984).

[18] J. Prost and J. Toner, Phys. Rev. A **36**, 5008 (1987).

[19] S. Pfeiffer, G. Heppke, D. S. Shankar Rao, and R. Shashidhar, Phys. Rev. A, **46**, 6166 (1992).

[20] M. Hosino, H. Nakano, and H. Kimura, J. Phys. Soc. Jpn. **46**, 1709 (1979).

[21] M. P. Allen, G. T. Evans, D. Frenkel, and B. M. Mulder, Adv. Chem. Phys. **86**, 1 (1994).

[22] J.-P. Hansen and I. R. McDonald, *Theory of Simple Liquids*, 2nd ed. (Academic, London, 1986).

[23] P. Tarazona, Philos. Trans R. Soc. London Ser. A **344**, 307 (1993).

[24] A. Poniewierksi, Phys. Rev. A **45**, 5605 (1992).

[25] M. Hosino, H. Nakano, and H. Kimura, J. Phys. Soc. Jpn. **47**, 740 (1979).

[26] W. M. Gelbart and B. Barboy, Acc. Chem. Res. **13**, 290 (1980).

[27] T. J. Sluckin, Liquid Crys. **6**, 111 (1989).

[28] G. J. Vroege and H. N. W. Lekkerkerker, Rep. Prog. Phys. **55**, 1241 (1992).

[29] T. M. Reed and K. E. Gubbins, *Applied Statistical Mechanics* (McGraw-Hill Kogakusha, Tokyo, 1973).

[30] R. P. Sear and G. Jackson, Mol. Phys. **82**, 473 (1994).

[31] R. B. Meyer and T. C. Lubensky, Phys. Rev. A **14**, 2307 (1976).

[32] J. A. C. Veerman and D. Frenkel, Phys. Rev. A **43**, 4334 (1990).